frontiers | Frontiers in Earth Science

TYPE Original Research
PUBLISHED 26 July 2022
DOI 10.3389/feart.2022.921264

OPEN ACCESS

EDITED BY
Steven L. Forman,
Baylor University, United States

REVIEWED BY
Nick Lancaster,
Desert Research Institute (DRI),
United States
Yu Li,
Lanzhou University, China

*CORRESPONDENCE
Kathryn E. Fitzsimmons,
kathryn.fitzsimmons@uni-tuebingen.de

SPECIALTY SECTION
This article was submitted to Quaternary Science, Geomorphology and Paleoenvironment,
a section of the journal
Frontiers in Earth Science

RECEIVED 15 April 2022
ACCEPTED 01 July 2022
PUBLISHED 26 July 2022

CITATION
Fitzsimmons KE and Gromov SS (2022), Northward expansion of the westerlies over glacial southeastern Australia: evidence from semi-arid lunette dunes, temperate basalt plains, and wind modelling.
Front. Earth Sci. 10:921264.
doi: 10.3389/feart.2022.921264

Northward expansion of the westerlies over glacial southeastern Australia: evidence from semi-arid lunette dunes, temperate basalt plains, and wind modelling

Kathryn E. Fitzsimmons[1]* and Sergey S. Gromov[2]

[1]Department of Geosciences, University of Tübingen, Tübingen, Germany, [2]Department of Atmospheric Chemistry, Max Planck Institute for Chemistry, Mainz, Germany

It has long been hypothesized that the last glacial maximum (LGM) oversaw cold, arid, windy climates across southern Australia, and that these were driven by intensification and northward expansion of mid-latitude westerly circulation. Moreover, it was recently suggested that Australia experienced an extended LGM which began several millennia before the global peak. Aeolian sedimentary deposits provide key evidence for these hypotheses, and climate modelling an alternative means to test them. As yet, however, combined approaches to reconstructing glacial environments on the continent are scarce. Here we provide new evidence for westerly wind regimes across glacial southeastern Australia. We confirm active transverse lunette deposition at c. 29 ka and c. 23–19 ka in the semi-arid Willandra Lakes, and identify aeolian sand incursions to Spring Creek on the temperate Western Victorian Volcanic Plains from c. 29 ka. The Spring Creek deposits contain a surprising quantity of sand-sized quartz given the basalt setting, which we propose to be allochthonous and likely transported some distance. The site lies more than 50 km east and south of dunefields which were active at the same time and may have contributed sediment via long distance transport. We investigate the hypothesis for northward glacial expansion of westerly winds by combining our sediment records with aeolian particle transport simulations. We find that LGM near-surface winds were dominated by stronger, more focussed westerly air flow across southeastern Australia, compared with presently more diffuse wind regimes. Our results suggest stronger potential for LGM eastward distal sand transport onto the basalt plains, coeval with enhanced aeolian activity in the semi-arid Australian dunefields. Our combined reconstruction of aeolian

Abbreviations: AMS, Accelerator Mass Spectrometry; CAM, Central Age Model; De, Equivalent dose; ECMWF, European Centre for Medium-range Weather Forecasting; FMM, Finite mixture model; GCM, General Circulation Model; ICP, Inductively coupled plasma; LGM, Last Glacial Maximum; MDB, Murray-Darling Basin; OSL, Optically stimulated luminescence; PD, Present day; RPL, Ram Paddock Lake; SAR, Single Aliquot Regenerative Dose Protocol; WPL, Well Paddock Lake; WVVP, Western Victorian Volcanic Plain

deposition and trajectory modelling confirms the extended LGM hypothesis and indicates a northward migration of westerly winds over southeastern Australia during this period.

KEYWORDS

aeolian transport, Australia, Willandra Lakes, Spring Creek megafauna site, western Victorian volcanic plains, last glacial maximum (LGM)

1 Introduction

The last glacial maximum (LGM) is defined as the coldest period of the last glacial stage, and oversaw global marine oxygen isotope maxima, sea level minima and maximum ice sheet extents (Lisiecki and Raymo, 2005; Clark et al., 2009; Lambeck et al., 2014). Whilst a global definition of the LGM, based on maximum ice volume and constrained to 26.5–19 ka (Clark et al., 2009), is widely accepted, a growing body of proxy and model evidence indicates that the timing and extent of the LGM varied around the planet (Rehfeld et al., 2018).

The arid continent of Australia diverges from the global mean in the spatial and temporal conditions of its LGM. Glaciation was limited in extent (Barrows et al., 2001; Barrows et al., 2002). Cooler temperatures instead brought expansion of more effectively arid conditions (Petherick et al., 2008; Fitzsimmons et al., 2013; Falster et al., 2018) and also oversaw increased runoff through reduced vegetation and evapotranspiration (Fitzsimmons et al., 2015; Hesse et al., 2018; Mueller et al., 2018). Recent studies have suggested that the inception of cooler, effectively drier conditions in Australia preceded the global LGM by several millennia, with a widespread shift dating to c. 29 ka (Petherick et al., 2017; Falster et al., 2018; Cadd et al., 2021).

In southern Australia, LGM conditions have been hypothesized to have been driven by northward expansion and intensification of the mid-latitude westerly winds (Hesse and McTainsh, 1999; Petherick et al., 2009; Shulmeister et al., 2016; Falster et al., 2018). In large part the hypothesis for westerly migration has been based on proxy evidence for aeolian sediment transport or moisture delivery. As yet, however, combining proxy information with trajectory models for sediment transport pathways remains poorly explored as a means to investigate the shifts in climate circulation responsible for driving the transition to LGM conditions.

In this study, we investigate the hypothesis for LGM northward migration of the mid-latitude westerlies over southeastern Australia using a combination of proxy and modelling approaches. We investigate the timing and sedimentology of transverse lunette dune building on the downwind (eastern) margins of two hitherto unstudied basins within the semi-arid Willandra Lakes system, within the context of existing chronostratigraphic frameworks for that region (Fitzsimmons et al., 2014; Fitzsimmons, 2017; Barrows et al., 2020; Jankowski et al., 2020). We also investigate the timing of deposition of sand-bearing sediments at the Spring Creek megafauna site on the temperate Western Victorian Volcanic Plain (WVVP), which contains an unexpectedly large proportion of sand-sized quartz for a basalt province. The Spring Creek case study provides an opportunity to explore the possibility of distal aeolian transport from dunefields further west as an indicator of enhanced westerly air flow, while simultaneously addressing a long-standing debate about the antiquity of megafaunal remains in the area (Flannery and Gott, 1984; White and Flannery, 1995; Porch and Kershaw, 2010). We interrogate the ages generated by our study for evidence supporting the hypothesis for an extended LGM in Australia. Finally, we compare our sedimentological datasets with simulations of aeolian particle transport for the present day (PD) and LGM, based on climate reanalysis and modelling respectively, in order to test the likelihood of glacial-age enhanced westerly circulation.

2 Materials and methods

2.1 Willandra Lakes localities and sampling

The Willandra Lakes are a presently dry chain of five large (and several smaller) lakes located in the Murray-Darling Basin (MDB) of semi-arid southeastern Australia, a system best known for its preservation of past hydrological, environmental and archaeological traces (Bowler, 1976; Fitzsimmons et al., 2014; Fitzsimmons et al., 2019; Barrows et al., 2020; Jankowski et al., 2020), including some of the earliest evidence for human occupation on the continent (Bowler, 1998; Bowler et al., 2003). The lakes were fed almost entirely by the Willandra Creek, a distributary of the Lachlan River which has its headwaters in the temperate highlands and which ceased to flow just after the LGM (Fitzsimmons et al., 2014). A number of lakes, including Leaghur and Durthong, represent through-flow basins; others, such as Lake Mungo, were overflow features (Bowler et al., 2012). The palaeohydrology of each lake is best recorded in the sediments and stratigraphy of its transverse shoreline dune (lunette) which lies immediately east and downwind of each individual basin (Bowler, 1983). The chronology and past environmental history of the Willandra lunettes, including evidence for oscillating lake filling and drying during the LGM (e.g., Bowler et al., 2012; Fitzsimmons et al., 2014; Jankowski et al., 2020) and a possible mega-lake event just prior to peak LGM (Fitzsimmons et al., 2015), has been described

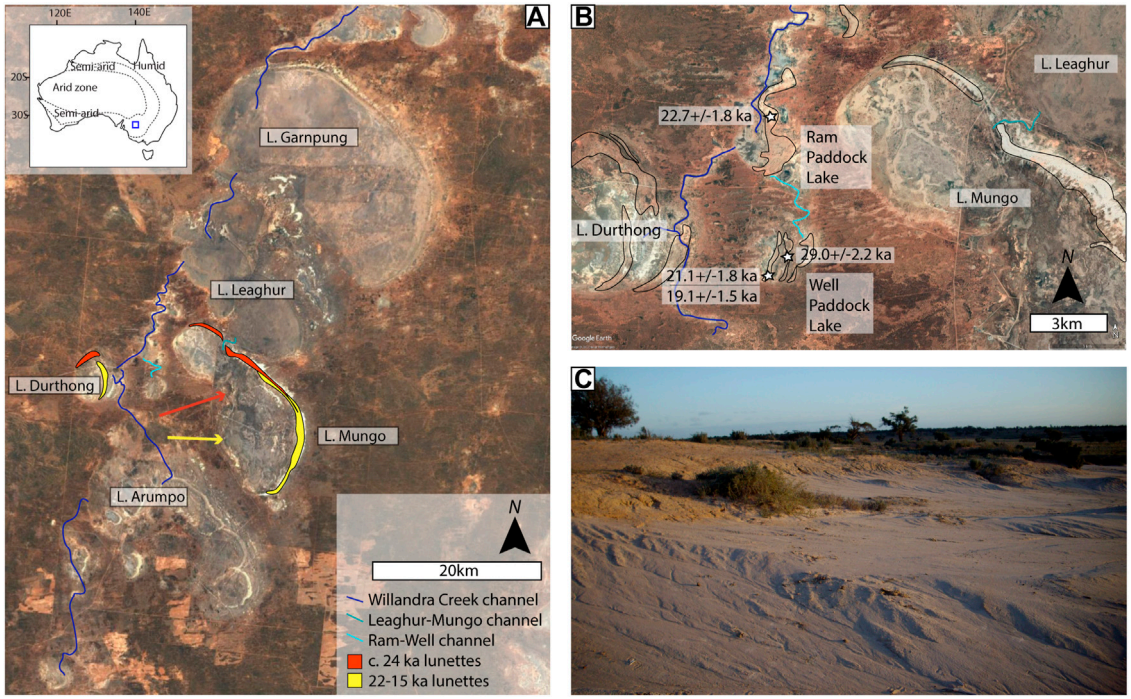

FIGURE 1
Location, context and chronology of RPL and WPL within the Willandra Lakes system. **(A)** Location of the Willandra Lakes in semi-arid southeastern Australia (inset) and the lakes system, including the Willandra Creek and interconnecting channels. The extent of maximum thickness of the c. 24 ka and 22–15 ka lunettes at Lakes Durthong and Mungo, along with the proposed prevailing wind vectors active during those depositional phases (Fitzsimmons, 2017), are also shown. **(B)** Local context, including lunette outlines, and chronology of the sampling sites at RPL and WPL. **(C)** The WPL inner lunette, photographed looking south. Base images sourced from Google Earth.

in the literature. In addition, it has been noted that the orientation of the lunettes varied through time (Fitzsimmons, 2017), on the basis of the assumption that the location of the thickest deposition along the lake margin represents the vector of the prevailing wind at the time. At c. 24 ka, this vector was west-south-westerly; over the period c. 22–15 ka, the prevailing winds were more directly westerly (Fitzsimmons, 2017).

In this study we investigate the timing of lunette deposition at two smaller, hitherto undocumented lakes within the Willandra system, located between Lakes Leaghur and Durthong (Figure 1A). Ram Paddock Lake (RPL) is a very low relief throughflow basin with a single low angle, broad, source-bordering lunette along its eastern margins (Figure 1B). A shallow, poorly defined channel connects RPL with Well Paddock Lake (WPL) to the south. WPL is an overflow basin, smaller but similar in setting to Lake Mungo upstream. WPL preserves several parallel lunette dunes which suggest a progressive decrease in lake volume over its lifetime (Figure 1B).

Sampling at RPL was undertaken by auger due to a lack of exposures and the low relief of its lunette. We selected a site which had experienced minimal surface disturbance by grazing and collected our optically stimulated luminescence (OSL) dating sample by hand auger according to published methods (Fitzsimmons et al., 2007). Following extensive foot survey of the geomorphology and stratigraphy of the WPL lunettes, we selected two sites (WELL6 and WELL14) for OSL sampling, one each from the inner and outer lunettes, where stratigraphy was exposed in small profiles. We collected three OSL samples at WPL by driving 10 cm long, 4 cm diameter stainless steel tubes horizontally into the profiles. Additional sediment was collected from around the sample holes for dose rate analysis. Further information about sample sites, coordinates and stratigraphy is provided in the Supplementary Information.

2.2 The Spring Creek locality and sampling

The Spring Creek site lies on the WVVP approximately 480 km south of the Willandra Lakes sites. The WVVP is the third largest basalt province in the world and although its climate is presently temperate, it lies east and south of extensive dunefields which were active in the past (Tumney, 2001; Lomax et al., 2011) (Figure 2A). The locality lies within a creek bed which has its headwaters on the slopes and lava flows of the Mt. Rouse volcano (Figure 2B), part of the Newer

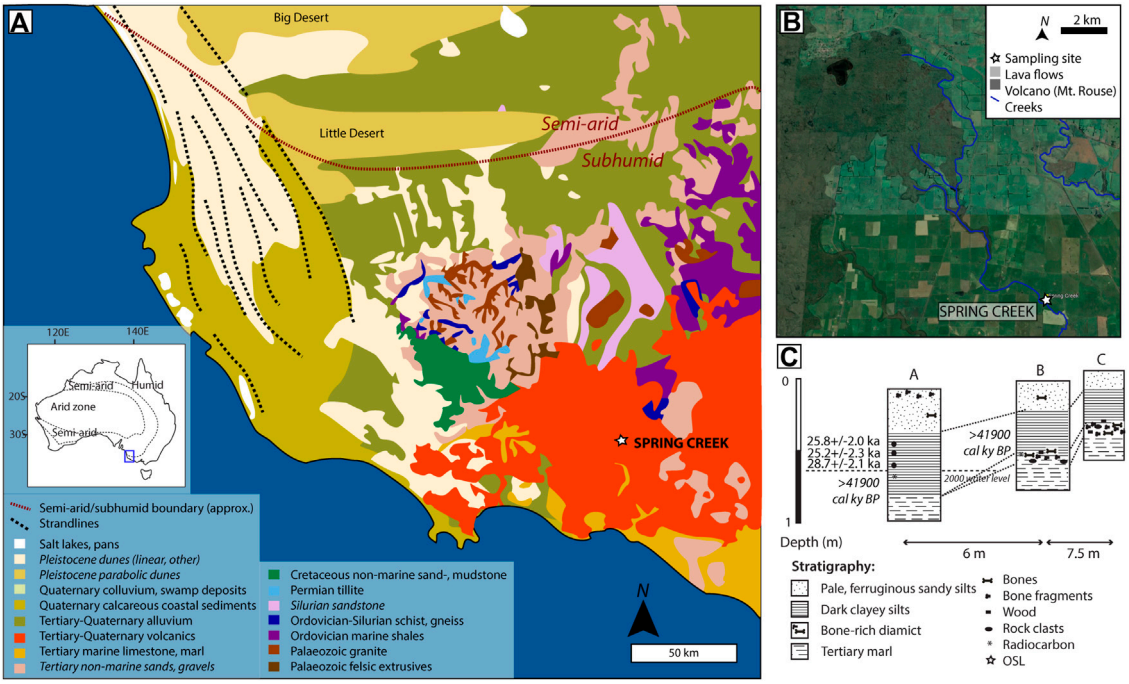

FIGURE 2
Location, geological context and chronology of the Spring Creek area. **(A)** Location of Spring Creek in southeastern Australia (inset) with respect to geology (Geological Survey of Victoria, 1982) and the approximate PD semi-arid/subhumid boundary (source: Bureau of Meteorology). Pleistocene strandlines and possible sources of sand which may have been transported to Spring Creek are shown in the legend in italics. **(B)** Local context of the Spring Creek site, showing the volcano Mt. Rouse and its most recent associated lava flows to the north and west, and the catchment of Spring Creek draining the basaltic surface. Base image sourced from Google Earth. **(C)** Stratigraphy and chronology of the sampled sections at Spring Creek, including stratigraphic setting of the bone diamict, OSL ages and summarized ^{14}C dates.

Volcanic Province with an eruption date of 284.4 ± 1.8 ka (Matchan and Phillips, 2014).

The Spring Creek locality initially gained attention as the site of proposed late survival of a number of extinct megafaunal species including *Macropus giganteus* and *Palorchestes* (Flannery and Gott, 1984). Subsequent direct accelerator mass spectrometry (AMS) radiocarbon dating of the bones suggested contamination by younger material (White and Flannery, 1995), later confirmed by infinite radiocarbon dates on plant and invertebrate samples (Porch and Kershaw, 2010) more consistent with the Australia-wide model for megafaunal extinction 46.4 ± 4.8 ka (Roberts et al., 2001). As yet, however, the depositional context of the site remained undated; this was the initial objective of our sampling at Spring Creek.

Sampling at Spring Creek focused on a profile (A) exposed c. 6–13 m downstream of the main bone deposit (profiles B and C; Figure 2C), where stratigraphy could be correlated. The stratigraphy comprises Tertiary marls unconformably underlying dark, organic-rich clayey silts, between which the bone-rich diamict is concentrated. The dark clayey silts are overlain by pale, ferruginous sandy silts; these could not reliably be sampled due to risk of collapse. We collected three samples from the dark clayey silts in the same manner as at WPL. The Supplementary contains additional stratigraphic information.

2.3 Luminescence dating

The Willandra Lakes OSL samples were processed and measured at the Department of Human Evolution, Max Planck Institute for Evolutionary Anthropology, Leipzig, Germany. These samples were processed using published procedures from nearby lunette sediments (Fitzsimmons et al., 2014). We extracted the 180–212 µm purified quartz fraction of each sample for measurement. Equivalent dose (D_e) measurements were made on 600 grains per sample using an automated Risø TL-DA-20 reader with a single grain laser attachment (Botter-Jensen, 1997; Botter-Jensen et al., 2000), adopting the single-aliquot regenerative dose (SAR) protocol (Murray and Wintle, 2000; Murray and Wintle, 2003). Preheat and cutheat temperatures of 260°C and 220°C respectively were applied based on tests made on samples from nearby sites (Fitzsimmons et al., 2014; Fitzsimmons, 2017). Single grain signals were accepted for D_e analysis following published criteria (Fitzsimmons et al., 2014). When

dose distributions exceeded 30% overdispersion, we calculated the final D_e using the Finite Mixture Model (FMM) (Galbraith and Green, 1990), otherwise we used the Central Age Model (CAM) (Galbraith et al., 1999). The beta, gamma and cosmic ray dose rates of the RPL and WPL samples were determined using laboratory beta counting; high resolution germanium gamma spectrometry undertaken at the "Felsenkeller" Laboratory (VKTA) in Dresden, Germany and converted to dose rates using published factors (Adamiec and Aitken, 1998); and published cosmic ray dose rate equations (Prescott and Hutton, 1994), respectively. Moisture contents of 5 ± 3% (Hesse, 2016) and published attenuation factors (Guérin et al., 2011) were used.

The Spring Creek OSL samples were processed and measured following published procedures (Fitzsimmons et al., 2007) at the Research School of Earth Sciences, Australian National University in Canberra, Australia. The purified 180–212 µm quartz was prepared as small (3 mm) aliquots for measurement since no single grain readers were available at the time; 24 aliquots were prepared for samples K1917 and K1918, and 12 aliquots from K1919 due to the limited amount of quartz recovered from this sample. No material remained following these measurements for subsequent single-grain analysis. D_e measurements were undertaken using the SAR protocol on automated Risø TL-DA-15 and TL-DA-12 readers equipped with blue light-emitting diodes for light stimulation (Botter-Jensen et al., 1999; Botter-Jensen et al., 2000). Preheat and cutheat temperatures of 260°C and 220°C respectively were used based on tests from nearby samples (Fitzsimmons et al., 2010). Since the dose distributions yielded normal distributions, we used the CAM for age calculation. Beta dose rates were determined from radioactive isotope concentrations measured using inductively-coupled plasma (ICP) mass spectrometry (U, Th) and ICP atomic emission spectrometry (K) analysed at Genalysis Laboratories (Perth, Australia) on homogenised subsamples; gamma dose rates were calculated from *in situ* gamma spectrometry; cosmic ray dose rates were calculated according to Prescott and Hutton (1994). Sediment moisture contents were close to saturation (28 ± 10%) given proximity to the creek. Dose rate attenuation was calculated based on published factors (Guérin et al., 2011).

Additional information relating to OSL sample processing and measurement is included in the Supplementary Information.

2.4 Modelling of wind regimes and aeolian particle transport

We used atmospheric general circulation model (GCM) product-aided PD and LGM reconstructions to investigate changes in surface wind regimes, dust transport pathways and potential source footprints to the Willandra Lakes and Spring Creek sites. Synoptic fields (6-hour resolution, 30-year continuous records) for PD conditions (1989–2018) were derived from the ERA INTERIM reanalysis dataset (Berrisford et al., 2011; Dee et al., 2011), available from the European Centre for Medium-Range Weather Forecasting (ECMWF). For the LGM state, we used a 6 h, 30-year output from the MPI-ESM-P model (r1i1p1-P experiment) which participated in the Climate Model Intercomparison Project, Phase 5 (Giorgetta et al., 2013). The MPI-ESM-P model was found to reproduce climate well against available surface proxy data (Pongratz et al., 2009), which can be considered an indicrect indication of the adequately reproduced general circulation by the model. The PD and LGM products differ in spatial resolution (0.75° vs. 1.88°, respectively); PD precipitation and 10 m wind gust data are based on forecast fields.

We calculated wind regime statistics from 10-metre winds sampled in respective model grid cells enclosing (not interpolating) the site locations. Wind direction-strength occurrence histograms were derived by season (summer/DJF, autumn/MAM, winter/JJA, spring/SON) and for the entire datasets (ANN). Dust transport and source footprint analyses were performed using the Lagrangian particle dispersion model FLEXPART (Stohl et al., 2005; Pisso et al., 2019), driven by respective GCM product synoptic data in the troposphere over the 125–145°E and 25–55°S domains. We simulated backward-in-time 48 h' transport of several million particles of 20, 60 and 120 µm sizes, accounting for removal processes (dry deposition and scavenging with precipitation, using properties of quartz) for the two sites' receptor locations for each synoptic term. Sensitivity simulations with dry and wet removal turned off indicate that these processes have negligible effect on the final results. Obtained particle density distributions in near-surface layers (up to 15 m) were then filtered according to our mobilization criteria (10 m wind gusts exceeding 5 m/s, land surface, no snow cover). We present our combined climatic distributions as total/seasonal shares of the annual transport-only mediated contribution of potential wind-mobilized dust source locations. We assumed a 120 m sea level reduction for LGM conditions, which results in footprints extending beyond the PD coastal lines.

3 Results

3.1 Luminescence chronologies

The OSL results for RPL, WPL and Spring Creek are summarized in Table 1. Published accelerator mass spectrometry (AMS) radiocarbon dates from Spring Creek (Porch and Kershaw, 2010) are included for comparison with the OSL ages.

The Willandra Lakes yield three ages conforming to the global LGM (26.5–19 ka; Clark et al., 2009), and one predating this by several millennia (29.0 ± 2.2 ka). The LGM-

TABLE 1 Chronological data. Supporting data and age estimates based on OSL dating for the RPL and WPL sites in the Willandra Lakes area, calculated on single grains of quartz. Supporting data and age estimates based on OSL dating of dark, laminated clayey silts at Spring Creek (Section A), undertaken on single aliquots of quartz. Results of AMS ^{14}C dating of organic remains (seeds, insects and pollen) from the base of the same horizon at Spring Creek (Sections A and B) (Porch and Kershaw, 2010), calibrated using SHCal20 (Hogg et al., 2020).

Sample	Depth (m)	D_e (Gy)	σ (%)	Attenuated dose rates (Gy/ka)			Total dose rate (Gy/ka)	Age (ka)
				Beta	Gamma	Cosmic		
Willandra Lakes sites—OSL ages								
Ram Paddock								
EVA1125	0.85 ± 0.05	30.4 ± 0.9[a]	16	0.75 ± 0.08	0.46 ± 0.05	0.13 ± 0.01	1.34 ± 0.10	22.7 ± 1.8
Well Paddock								
EVA1126	0.40 ± 0.05	31.6 ± 1.3[a]	35	0.95 ± 0.10	0.56 ± 0.06	0.14 ± 0.01	1.65 ± 0.11	19.1 ± 1.5
EVA1127	0.30 ± 0.05	22.9 ± 0.55[b]	20	0.58 ± 0.06	0.36 ± 0.04	0.14 ± 0.01	1.09 ± 0.09	21.1 ± 1.8
EVA1128	0.35 ± 0.05	36.1 ± 0.70[b]	23	0.71 ± 0.07	0.39 ± 0.04	0.14 ± 0.01	1.24 ± 0.09	29.0 ± 2.2
Spring Creek site—section A OSL ages								
K1917	0.22 ± 0.02	32.7 ± 1.7[b]	23	0.66 ± 0.07	0.50 ± 0.05	0.11 ± 0.01	1.27 ± 0.07	25.8 ± 2.0
K1918	0.31 ± 0.02	36.2 ± 1.6[b]	18	0.63 ± 0.06	0.52 ± 0.05	0.11 ± 0.01	1.26 ± 0.06	28.7 ± 2.1
K1919	0.27 ± 0.02	36.0 ± 2.2[b]	20	0.79 ± 0.08	0.53 ± 0.05	0.11 ± 0.01	1.43 ± 0.08	25.2 ± 2.3

Spring Creek site—radiocarbon dates

Section	Sample	Material			Uncalibrated date (ky BP)	Calibrated date (cal ky BP)
A	SC97/5A	*Pimelea sp.* Seeds			BG (>46300)	>46639
	SC97/5B	Beetle sclerites	>44100	>44399		
	SC97/5C	Pollen preparation	37400 ± 1100	41927		
B	SC97/6A	*Pimelea sp.* Seeds			44900 ± 3600	>45347
	SC97/6B	Beetle sclerites	BG (>43400)	>43769		
	SC97/6C	Pollen preparation	39600 ± 1400	41924 ± 2039		
	SC97/6D	Asteraceae seeds	43400 ± 2100	45809 ± 4764		

[a]Equivalent doses calculated using the FMM of Galbraith and Green (1990); overdispersion (σ) values refer to σ of the final accepted age population.
[b]Equivalent doses calculated using the CAM of Galbraith et al. (1999).

age results indicate active accumulation of sandy clay material to the lunette at RPL, with the sedimentology reflecting periodic filling and drying associated with intermittent Willandra Creek flow. The two LGM ages at the overflow lake, WPL, derive from both sandy and clayey sediments from its inner lunette and likewise suggest oscillating water levels. Both the timing and sediments associated with this phase correlate with the so-called Arumpo unit of oscillating lake filling and drying observed in other Willandra basins (mean age 21.8 ± 3.4 ka; Fitzsimmons et al., 2015), and which represents the final phase of lake filling before the Willandra Creek ceased to flow (Fitzsimmons et al., 2019). The c. 29 ka age for the alternating sands and clayey sands of the WPL outer lunette predates inner lunette deposition. We consider all ages to be robust and the quartz suited to OSL dating, based on bright, rapidly decaying signals, exponential dose-response curves, recycling ratios close to unity, minimal IRSL signals, thermal transfer of charge and sensitivity change through the SAR cycles.

The Spring Creek samples all lie within 2σ error and correspond to the period preceding the global LGM; they do conform to the Australian extended LGM (Cadd et al., 2021). Whilst the Spring Creek sediments are not rich in sand-sized quartz, all aliquots exhibit optimal signals for luminescence dating. All samples yield bright, rapidly decaying signals

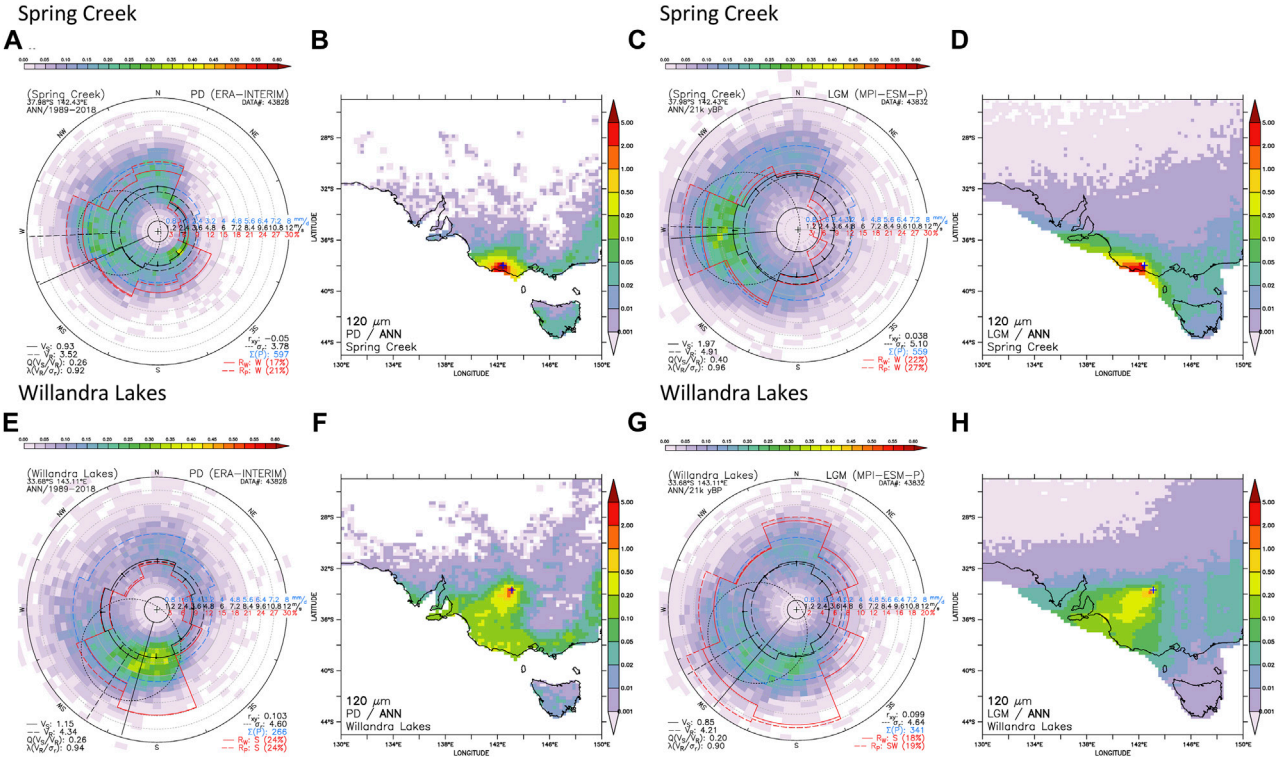

FIGURE 3
Wind regime analysis and simulated aeolian sources and transport statistics, and implications for air mass circulation in the PD and LGM. See Section 2.4 and Supplementary Figures for detailed description of tabled parameters. Color scales show relative contribution to the annual totals at a given site. **(A)** Annual wind direction-strength occurrence histogram for the PD at Spring Creek. **(B)** Modelled source footprint of mobilized dust transport of 120 μm particles to Spring Creek in the PD. **(C,D)** Results for the LGM conditions at Spring Creek. **(E,F)** Results for the PD at the Willandra Lakes. **(G,H)** Results for the LGM conditions at the Willandra Lakes. **(I)** PD circulation of major air masses Sm (southern maritime; westerlies) and sTc (subtropical continental; northerlies) to southeastern Australia (after Tapper and Hurry, 1993). **(J)** Proposed circulation to southeastern Australia during the LGM based on our simulations, indicating stronger and northward migration of westerly airflow over the continent.

typical of strongly sensitive quartz dominated by the fast component, recycle well, and produce negligible IRSL signals, thermal transfer and minimal sensitivity change. Our results indicate that the sediment comprising the dark clayey silt unit was deposited relatively rapidly over the millennia c. 29–25 ka. The organic-rich clayey silts from which the three samples were collected appear to derive from a mixture of Tertiary marls, likely reworked from upstream, integrated with fine-grained basalt eroded from the Mt Rouse and surrounding earlier lava flows. It is unlikely, however, that either of these parent materials contributed much sand-sized quartz to the deposited sediment—particularly in the case of the uppermost pale sandy silt unit. We propose that at least some of the quartz is allochthonous and aeolian in nature. This hypothesis may be supported—although not diagnostic—by the bright OSL signals observed in our samples, since volcanic quartz in particular does not produce a useful signal for conventional OSL dating (Tsukamoto et al., 2007).

3.2 Comparison of modern and modelled last glacial maximum wind regimes

The full suite of wind regime statistics and particle transport/wind-mobilized sources footprint simulations for both PD and LGM at both sites is presented in the Supplementary Information. The annual wind regime statistics and source footprints are summarized in Figure 3.

In the Willandra Lakes region, the PD wind regime is strongly southerly, particularly in the autumn and summer months, and weaker westerly winds are persistent in winter and spring. A northerly wind vector is also observed in the winter months. By contrast, the modelled LGM wind regimes indicate stronger winds and hence transport distances. The strongest LGM winds were southerlies in the summer (and to a lesser extent autumn) months, whereas the spring months oversaw reasonably strong south-westerly air flow and winter winds were more diffuse, spanning the westerly through to

northerly quadrant. Our modelling of likely particle trajectories for both time slices yielded grain-size dependent results. In the PD, finer (20 μm) grain sizes are most likely derived from local sources irrespective of season, as evidenced by the small FLEXPART footprint (Supplementary Figure S11). By comparison, the footprint for LGM finer-grained transport is larger and most likely derives predominantly from the WSW (Supplementary Figure S17). The simulations for both 60 and 120 μm particle transport yield similar results. The footprints for these grain-sizes are substantially larger, and the likelihood of distal transport is greatest in the autumn, winter and summer months; source areas span the south-western quadrant.

At Spring Creek, we observe a weaker and more diffuse PD wind regime compared with the Willandra region. Overall, westerly air flow is most persistent, although the strongest winds are south-easterlies experienced in the summer and northerlies in the winter months. The strongest westerly winds occur in the spring months. By comparison, westerly airflow is both stronger and more dominant in the LGM simulation. The westerlies are particularly strong during the LGM spring months; these were coupled with a northerly component during the winter and a southerly vector in the summers. Our footprint analysis for Spring Creek in the PD suggests a somewhat smaller potential source region for finer (20 μm) grains than for the Willandra area, but still larger than for the coarser grain-sizes. Finer grains most likely derive from the proximity of Spring Creek, with probability decreasing with distance irrespective of direction. Both coarser grain sizes (60 and 120 μm) yield similar results and suggest that most of this size material derives from the west, south and east, irrespective of season. The LGM simulations yield a larger footprint for the 20 μm fraction than for the PD and suggest substantial transport from the west, particularly in spring, summer and winter. This strong eastward transport vector is reflected in the simulations for the coarser grain sizes and suggests a high probability of westerly LGM transport of sand-sized material in all seasons, over a footprint which extends more than 170 km to what is now the South Australian coast.

4 Discussion

4.1 Glacial age palaeoenvironments in southeastern Australia

Our results from the Willandra Lakes corroborate previously published chronologies from the lake system, which indicate oscillating lake levels from late OIS 3 into the peak LGM (Fitzsimmons et al., 2014; Fitzsimmons et al., 2015; Barrows et al., 2020; Jankowski et al., 2020). Our c. 23 ka age from RPL indicates that flow was at least intermittently active in the Willandra Creek at the time of lunette building in neighbouring Lakes Durthong and Mungo (Fitzsimmons, 2017). At WPL, inner lunette construction c. 21–19 ka corresponds to the final phases of accumulation in the adjacent basins (Bowler et al., 2012). Our c. 29 ka age for the outer lunette at WPL records sediment accumulation which slightly postdates the oscillating lake conditions of the Upper Mungo unit in central Lake Mungo (Fitzsimmons et al., 2014), but nevertheless corresponds to the earlier part of the extended LGM unit (LU4-9) dated in the southern part of the lunette (Jankowski et al., 2020). Whilst it is unclear precisely which phase this oldest WPL age corresponds to, it nevertheless aligns with the general chronologic framework for the Willandra Lakes.

At Spring Creek, the presence and age of sand-sized quartz in the dated clayey silt unit, which increases in concentration in the overlying pale sandy unit, presents an intriguing hypothesis. Whilst we cannot exclude the possibility that the Tertiary marls contributed quartz grains to these sediments, the particularly high concentrations of sandy quartz in the upper unit strongly suggests an increasing contribution to the basalt catchment of allochthonous material through time. Such material within a largely basaltic catchment is most likely to have been aeolian in origin. The influx of these sands began at c. 29 ka and corresponds to the initiation of increasing effective aridity at nearby Lake Surprise (Falster et al., 2018). To the west (and upwind), an increase in aeolian activity within subparabolic and linear dunes (Lomax et al., 2011), and downwind of major palaeoshorelines (Darrénougué et al., 2009; Fitzsimmons and Barrows, 2012), likewise dates from c. 30 ka or shortly thereafter. Whilst we cannot confirm the timing of deposition of the sandy upper unit, we propose that it represents an increasingly windy period associated with distal aeolian transport, which may be coeval with LGM peak effective aridity as recorded elsewhere in the region.

Our data support the emerging critical mass of proxy evidence suggesting that the initiation of the LGM in Australia preceded the global LGM (c. 26.5–19 ka; Clark et al., 2009) by several millennia (c. 29 ka; Petherick et al., 2008; Petherick et al., 2017; Cadd et al., 2021). The LGM was heralded by cooler climates and a decline in biological productivity across the continent (Petherick et al., 2017; Cadd et al., 2021), as well as an increase in indicators for aridity, windiness, or both, such as dune reactivation in the arid centre (Fitzsimmons et al., 2013; Hesse, 2016) and semi-arid southeast (Tumney, 2001; Lomax et al., 2011; Barrows et al., 2020), and increased aeolian influx to eastern Australia (Petherick et al., 2017). In the Murray-Darling Basin where the Willandra Lakes are situated, increased river discharge from c. 30 ka is thought to have been driven not only by cooler temperatures but also higher runoff ratios, lower evapotranspiration and reduced vegetation cover (Hesse et al., 2018; Mueller et al., 2018). A shift to such regimes is likely what drove the oscillating lake levels in the Willandra system over the extended Australian LGM.

4.2 Implications for last glacial maximum atmospheric circulation over southeastern Australia

Our results support the emerging body of data which argue for an extended LGM on the Australian continent compared with the global average (Petherick et al., 2017; Cadd et al., 2021). Cooler temperatures over this extended LGM in Australia manifested in the form of increased aeolian activity (Fitzsimmons et al., 2013), decreased biological productivity (Falster et al., 2018; Cadd et al., 2021 and references therein), and increased runoff in hydrological systems (Hesse et al., 2018; Mueller et al., 2018); it has been proposed that increased effective aridity, lower evapotranspiration, and possibly increased windiness contributed to these earth-surface responses. Our data from Spring Creek in particular argue for substantial aeolian incursions across the WVVP during this time period, so supporting an argument for increased wind strength during at least the early part of the extended Australian LGM. Under this proposed scenario, the most likely source areas for the sand-sized aeolian quartz are the Pleistocene parabolic and linear dunes which lie at least 50 km west of the Spring Creek site, and which oversaw aeolian reactivation from c. 30 ka (Lomax et al., 2011; Fitzsimmons and Barrows, 2012).

Our simulations of likely aeolian trajectories of quartz particles during the LGM provide a novel means by which to test the hypothesis for increased windiness over southeastern Australia during this time period (Figure 3D; Supplementary Material). Focussing on the Spring Creek site, we find a strong likelihood for the eastward transport of sand-sized (60 and 120 μm) material in a catchment extending at least 170 km west of the locality (Figure 3D). The longest-distance trajectory envelopes and highest probability of distal sand transport for these coarser grain sizes were found for the summer and autumn months (Supplementary Figures S21, S22). These are also most likely to have been the driest seasons and therefore these results are consistent with both a greater availability of sand at the source area—here assumed to be the sand dunes to the west—and with greater aeolian transport potential. All seasons have a westerly component to the wind regime (Supplementary Figure S10). Pleistocene aeolian sediments dominate the surface geology of that spatial envelope (Figure 2A), and provide additional support for the argument for increased LGM wind strength and associated aeolian transport.

We also considered whether seasonality may have played a role in the availability and transport of sand-sized particles to the Willandra Lakes lunettes during the LGM (Supplementary Figures S18, S19). Our reconstructions of wind regimes in the Willandra region during this time indicate the strongest winds, and those most consistent with the lunette orientations, fall within the winter and spring months (Supplementary Figure S9). Longer distance coarse-grained sand transport was more likely during the summer months (Supplementary Figures S18, S19), however since proximal transport was persistent throughout the year and we assume most lunette material to be locally derived from the respective lake basins, the seasonality of the trajectory envelopes would appear to play less of a role in lunette orientation in this region.

The most likely mechanism for increased LGM windiness over south-southeastern Australia is a more northward placement of the mid-latitude westerly wind systems compared with the present day (Figures 3I,J). This scenario matches both our proxy and modelled data, and supports earlier records of increased aeolian sediment flux off the east coast of the continent (Hesse and McTainsh, 1999; Petherick et al., 2009) and lake-marginal lunette building further north than is generally recorded (Shulmeister et al., 2016). It has been argued that cooling sea-surface temperatures in the Southern Ocean to the south of our sites during the extended LGM (Lopes dos Santos et al., 2013) may have influenced airflow and onshore delivery of precipitation to the continent, resulting not only in effectively drier conditions but also less impediment to westerly airflow due to the northward migration of subantarctic cold fronts (Falster et al., 2018). At larger scales, it has also been proposed that stronger westerly winds in the southern hemisphere mid-latitudes coincided with millennial-scale southward shifts of the intertropical convergence zone (ITCZ) coincident with short-lived northern hemisphere Heinrich cooling events (Whittaker et al., 2011). Our combined proxy-modelling approach reinforces this hypothesis and provides a more robust framework for investigating environmental archives for an extended LGM which oversaw increased windiness associated with northward migration of the westerly circulation.

Data availability statement

The datasets presented in this study can be found in online repositories. The names of the repository/repositories and accession number(s) can be found in the article/Supplementary Material.

Author contributions

KF conceived of the presented ideas in this study. KF undertook fieldwork and sampling at both Spring Creek and the Willandra Lakes. Analysis and interpretation of the chronological results was undertaken by KF; analysis and interpretation of the climate reanalysis and modelling results was undertaken by SG. KF wrote the first draft of the manuscript. Both authors contributed to manuscript revision, read and approved the submitted version.

Funding

Fieldwork at the Willandra Lakes was undertaken with the permission of the Elders' Council and the Technical and Scientific

Advisory Committee of the Willandra Lakes Region World Heritage Area (WLRWHA), and was funded by an Australian Research Council (ARC) Discovery Project (DP1092966). Associated laboratory analyses were supported by the Max Planck Institute for Evolutionary Anthropology. Fieldwork and laboratory analyses of the Spring Creek samples was funded by the household budget of the Luminescence Dating Laboratory, Research School of Earth Sciences, Australian National University. Past climate reconstructions were supported through the project PalMod funded by the German Federal Ministry of Education and Research (BMBF), Grant Nos. 01LP1921A and 01LP1921B. Resources for computer simulations and reanalysis data processing were provided by the German Climate Computing Centre (DKRZ) granted by its Scientific Steering Committee (WLA) under Project ID bm1030.

Acknowledgments

We acknowledge the deep and continued connection held by the Djabwurrung and Gunditjmarra First Nations people to Country around the Spring Creek area, and by the Paakantyi/Barkindji, Ngiyampaa and Mutthi people to Country around the Willandra Lakes World Heritage Area. We also thank the Whitehead family of the Spring Creek property for access to the site for sampling, and Nicholas Porch for assistance with the sampling at that locality. Thank you to the many Honours students of the Mungo Archaeology Project, directed by Nikki Stern, for their help in the field at RPL and WPL, and to Eva Reynolds and Steffi Hesse for their assistance with luminescence dating sample preparation. Thanks also to the two anonymous reviewers whose positive and constructive comments improved the manuscript. In memory of Lynda Petherick, colleague, friend and proponent of the extended Australian LGM hypothesis. Deep peace to you.

Conflict of interest

The authors declare that the research was conducted in the absence of any commercial or financial relationships that could be construed as a potential conflict of interest.

Publisher's note

Supplementary material

The Supplementary Material for this article can be found online at: https://www.frontiersin.org/articles/10.3389/feart.2022.921264/full#supplementary-material

References

Adamiec, G., and Aitken, M. (1998). Dose-rate conversion factors: Update. *Anc. TL* 16 (2), 37–50.

Barrows, T. T., Stone, J. O., Fifield, L. K., and Creswell, R. G. (2001). Late Pleistocene glaciation of the kosciuszko massif, snowy mountains, Australia. *Quat. Res.* 55 (2), 179–189. doi:10.1006/qres.2001.2216

Barrows, T. T., Stone, J. O., Fifield, L. K., and Creswell, R. G. (2002). The timing of the last glacial maximum in Australia. *Quat. Sci. Rev.* 21 (1-3), 159–173. doi:10.1016/s0277-3791(01)00109-3

Barrows, T. T., Fitzsimmons, K. E., Mills, S. C., Tumney, J., Pappin, D., Stern, N., et al. (2020). Late Pleistocene lake level history of lake Mungo, Australia. *Quat. Sci. Rev.* 238, 106338. doi:10.1016/j.quascirev.2020.106338

Berrisford, P., Dee, D. P., Poli, P., Brugge, R., Mark, F., Manuel, F., et al. (2011). *The ERA-Interim archive Version 2.0.* Shinfield Park, Reading: ECMWF.

Botter-Jensen, L., Mejdahl, V., and Murray, A. S. (1999). New light on OSL. *Quat. Sci. Rev.* 18 (2), 303–309. doi:10.1016/s0277-3791(98)00063-8

Botter-Jensen, L., Bulur, E., Duller, G. A. T., and Murray, A. S. (2000). Advances in luminescence instrument systems. *Radiat. Meas.* 32, 523–528. doi:10.1016/s1350-4487(00)00039-1

Botter-Jensen, L. (1997). Luminescence techniques: Instrumentation and methods. *Radiat. Meas.* 27, 749–768. doi:10.1016/s1350-4487(97)00206-0

Bowler, J. M., Johnston, H., Olley, J. M., Prescott, J. R., Roberts, R. G., Shawcross, W., et al. (2003). New ages for human occupation and climatic change at Lake Mungo, Australia. *Nature* 421 (6925), 837–840. doi:10.1038/nature01383

Bowler, J., Gillespie, R., Johnston, H., and Boljkovac, K. (2012). "Wind v water: Glacial maximum records from the Willandra Lakes," in *Peopled landscapes: Archaeological and biogeographic approaches to landscapes*. Editors S. Haberle, and B. David (Canberra: The Australian National University), 271–296.

Bowler, J. M. (1976). Aridity in Australia: Age, origins and expression in aeolian landforms and sediments. *Earth. Sci. Rev.* 12, 279–310. doi:10.1016/0012-8252(76)90008-8

Bowler, J. M. (1983). Lunettes as indices of hydrologic change: A review of the Australian evidence. *Proc. R. Soc. Vic.* 95, 147–168.

Bowler, J. M. (1998). Willandra lakes revisited: Environmental framework for human occupation. *Archaeol. Ocean.* 33, 120–155. doi:10.1002/j.1834-4453.1998.tb00414.x

Cadd, H., Petherick, L., Tyler, J., Herbert, A., Cohen, T. J., Sniderman, K., et al. (2021). A continental perspective on the timing of environmental change during the last glacial stage in Australia. *Quat. Res.* 102, 5–23. doi:10.1017/qua.2021.16

Clark, P. U., Dyke, A. S., Shakun, J. D., Carlson, A. E., Clark, J., Wohlfarth, B., et al. (2009). The last glacial maximum. *Science* 325 (5941), 710–714. doi:10.1126/science.1172873

Darrénougué, N., De Deckker, P., Fitzsimmons, K. E., Norman, M. D., Reed, L., van der Kaars, S., et al. (2009). A late Pleistocene record of aeolian sedimentation in blanche cave, naracoorte, south Australia. *Quat. Sci. Rev.* 28 (25-26), 2600–2615. doi:10.1016/j.quascirev.2009.05.021

Dee, D. P., Uppala, S. M., Simmons, A. J., Berrisford, P., Poli, P., Kobayashi, S., et al. (2011). The ERA-interim reanalysis: Configuration and performance of the data assimilation system. *Q. J. R. Meteorol. Soc.* 137 (656), 553–597. doi:10.1002/qj.828

Falster, G., Tyler, J., Grant, K., Tibby, J., Turney, C., Löhr, S., et al. (2018). Millennial-scale variability in south-east Australian hydroclimate between 30, 000 and 10, 000 years ago. *Quat. Sci. Rev.* 192, 106–122. doi:10.1016/j.quascirev.2018.05.031

Fitzsimmons, K. E., and Barrows, T. T. (2012). Late Pleistocene aeolian reactivation downwind of the Naracoorte East range, southeastern South Australia. *Z. für Geomorphol.* 56 (2), 225–237. doi:10.1127/0372-8854/2012/0068

Fitzsimmons, K. E., Rhodes, E. J., Magee, J. W., and Barrows, T. T. (2007). The timing of linear dune activity in the Strzelecki and Tirari Deserts, Australia. *Quat. Sci. Rev.* 26, 2598–2616. doi:10.1016/j.quascirev.2007.06.010

Fitzsimmons, K. E., Rhodes, E. J., and Barrows, T. T. (2010). OSL dating of southeast Australian quartz: A preliminary assessment of luminescence characteristics and behaviour. *Quat. Geochronol.* 5, 91–95. doi:10.1016/j.quageo.2009.02.009

Fitzsimmons, K. E., Cohen, T. J., Hesse, P. P., Jansen, J., Nanson, G. C., May, J.-H., et al. (2013). Late quaternary palaeoenvironmental change in the Australian drylands: A synthesis. *Quat. Sci. Rev.* 74, 78–96. doi:10.1016/j.quascirev.2012.09.007

Fitzsimmons, K. E., Stern, N., and Murray-Wallace, C. V. (2014). Depositional history and archaeology of the central Lake Mungo lunette, Willandra Lakes, southeast Australia. *J. Archaeol. Sci.* 41, 349–364. doi:10.1016/j.jas.2013.08.004

Fitzsimmons, K. E., Stern, N., Murray-Wallace, C. V., Truscott, W., and Pop, C. (2015). The Mungo mega-lake event, semi-arid Australia: Non-linear descent into the last ice age, implications for human behaviour. *PLoS ONE* 10(6), e0127008. doi:10.1371/journal.pone.0127008

Fitzsimmons, K. E., Spry, C., and Stern, N. (2019). Holocene and recent aeolian reactivation of the Willandra Lakes lunettes, semi-arid southeastern Australia. *Holocene* 29 (4), 606–621. doi:10.1177/0959683618824790

Fitzsimmons, K. E. (2017). Reconstructing palaeoenvironments on desert margins: New perspectives from Eurasian loess and Australian dry lake shorelines. *Quat. Sci. Rev.* 171, 1–19. doi:10.1016/j.quascirev.2017.05.018

Flannery, T., and Gott, B. (1984). The Spring Creek locality, southwestern Victoria, a late surviving megafaunal assemblage. *Aust. Zool.* 21 (4), 385–422.

Galbraith, R. F., and Green, P. F. (1990). Estimating the component ages in a finite mixture. *Int. J. Radiat. Appl. Instrum. Part D. Nucl. Tracks Radiat. Meas.* 17, 197–206. doi:10.1016/1359-0189(90)90035-v

Galbraith, R. F., Roberts, R. G., Laslett, G. M., Yoshida, H., and Olley, J. M. (1999). Optical dating of single and multiple grains of quartz from Jinmium rock shelter, northern Australia. Part 1, Experimental design and statistical models. *Archaeometry* 41, 339–364. doi:10.1111/j.1475-4754.1999.tb00987.x

Giorgetta, M. A., Jungclaus, J., Reick, C. H., Legutke, S., Bader, J., Böttinger, M., et al. (2013). Climate and carbon cycle changes from 1850 to 2100 in MPI-ESM simulations for the Coupled Model Intercomparison Project phase 5. *J. Adv. Model. Earth Syst.* 5 (3), 572–597. doi:10.1002/jame.20038

Guérin, G., Mercier, N., and Adamiec, G. (2011). Dose-rate conversion factors: Update. *Anc. TL* 29 (1), 5–8.

Hesse, P. P., and McTainsh, G. H. (1999). Last glacial maximum to early holocene wind strength in the mid-latitudes of the southern hemisphere from aeolian dust in the tasman sea. *Quat. Res.* 52 (3), 343–349. doi:10.1006/qres.1999.2084

Hesse, P. P., Williams, R., Ralph, T. J., Fryirs, K. A., Larkin, Z. T., Westaway, K. E., et al. (2018). Palaeohydrology of lowland rivers in the Murray-Darling Basin, Australia. *Quat. Sci. Rev.* 200, 85–105. doi:10.1016/j.quascirev.2018.09.035

Hesse, P. P. (2016). How do longitudinal dunes respond to climate forcing? Insights from 25 years of luminescence dating of the Australian desert dunefields. *Quat. Int.* 410 (B), 11–29. doi:10.1016/j.quaint.2014.02.020

Hogg, A. G., Heaton, T. J., Hua, Q., Palmer, J. G., Turney, C. S., Southon, J., et al. (2020). SHCal20 Southern Hemisphere calibration, 0–55, 000 years cal BP. *Radiocarbon* 62 (4), 759–778. doi:10.1017/rdc.2020.59

Jankowski, N. R., Stern, N., Lachlan, T. J., and Jacobs, Z. (2020). A high-resolution late Quaternary depositional history and chronology for the southern portion of the Lake Mungo lunette, semi-arid Australia. *Quat. Sci. Rev.* 233, 106224. doi:10.1016/j.quascirev.2020.106224

Lambeck, K., Rouby, H., Purcell, A., Sun, Y., and Sambridge, M. (2014). sea level and global ice volumes from the last glacial maximum to the holocene. *Proc. Natl. Acad. Sci. U. S. A.* 111 (43), 15296–15303. doi:10.1073/pnas.1411762111

Lisiecki, L. E., and Raymo, M. E. (2005). A Pliocene-Pleistocene stack of 57 globally distributed benthic 18O records. *Paleoceanography* 20 (1), PA1003. doi:10.1029/2004pa001071

Lomax, J., Hilgers, A., and Radtke, U. (2011). Palaeoenvironmental change recorded in the palaeodunefields of the Western Murray Basin, South Australia - new data from single grain OSL-dating. *Quat. Sci. Rev.* 30 (5-6), 723–736. doi:10.1016/j.quascirev.2010.12.015

Lopes dos Santos, R. A., Spooner, M. I., Barrows, T. T., De Deckker, P., Sinninghe Damsté, J. S., Schouten, S., et al. (2013). Comparison of organic (UK'37, TEXH86, LDI) and faunal proxies (foraminiferal assemblages) for reconstruction of late Quaternary sea surface temperature variability from offshore southeastern Australia. *Paleoceanography* 28 (3), 377–387. doi:10.1002/palo.20035

Matchan, E. L., and Phillips, D. (2014). High precision multi-collector 40Ar/39Ar dating of young basalts: Mount Rouse volcano (SE Australia) revisited. *Quat. Geochronol.* 22, 57–64. doi:10.1016/j.quageo.2014.02.005

Mueller, D., Jacobs, Z., Cohen, T. J., Price, D. M., Reinfelds, I. V., Shulmeister, J., et al. (2018). Revisiting an arid LGM using fluvial archives: A luminescence chronology for palaeochannels of the murrumbidgee river, south-eastern Australia. *J. Quat. Sci.* 33 (7), 777–793. doi:10.1002/jqs.3059

Murray, A. S., and Wintle, A. G. (2000). Luminescence dating of quartz using an improved single-aliquot regenerative-dose protocol. *Radiat. Meas.* 32 (1), 57–73. doi:10.1016/s1350-4487(99)00253-x

Murray, A. S., and Wintle, A. G. (2003). The single aliquot regenerative dose protocol: Potential for improvements in reliability. *Radiat. Meas.* 37 (4-5), 377–381. doi:10.1016/s1350-4487(03)00053-2

Petherick, L., McGowan, H., and Moss, P. (2008). Climate variability during the last glacial maximum in eastern Australia: Evidence of two stadials? *J. Quat. Sci.* 23 (8), 787–802. doi:10.1002/jqs.1186

Petherick, L. M., McGowan, H. A., and Kamber, B. S. (2009). Reconstructing transport pathways for late Quaternary dust from eastern Australia using the composition of trace elements of long traveled dusts. *Geomorphology* 105 (1-2), 67–79. doi:10.1016/j.geomorph.2007.12.015

Petherick, L. M., Moss, P. T., and McGowan, H. A. (2017). An extended last glacial maximum in subtropical Australia. *Quat. Int.* 432, 1–12. doi:10.1016/j.quaint.2015.11.015

Pisso, I., Sollum, E., Grythe, H., Kristiansen, N. I., Cassiani, M., Eckhardt, S., et al. (2019). The Lagrangian particle dispersion model FLEXPART version 10.4. *Geosci. Model Dev.* 12 (12), 4955–4997. doi:10.5194/gmd-12-4955-2019

Pongratz, J., Reick, C. H., Raddatz, T., and Claussen, M. (2009). Effects of anthropogenic land cover change on the carbon cycle of the last millennium. *Glob. Biogeochem. Cycles* 23. doi:10.1029/2009gb003488

Porch, N., and Kershaw, A. P. (2010). "Comparative AMS 14C dating of plant macrofossils, beetles and pollen preparations from two late Pleistocene sites in southeastern Australia," in *Altered Ecologies (Terra Australis 32): Fire, climate and human influence on terrestrial landscapes*. Editors S. Haberle, J. Stevenson, and M. Prebble (Canberra: Australian National University EPress), 395–403.

Prescott, J. R., and Hutton, J. T. (1994). Cosmic ray contributions to dose rates for luminescence and ESR dating: Large depths and long-term time variations. *Radiat. Meas.* 23 (2-3), 497–500. doi:10.1016/1350-4487(94)90086-8

Rehfeld, K., Münch, T., Ho, S. L., and Laepple, T. (2018). Global patterns of declining temperature variability from the last glacial maximum to the holocene. *Nature* 554, 356–359. doi:10.1038/nature25454

Roberts, R. G., Flannery, T. F., Ayliffe, L. K., Yoshida, H., Olley, J. M., Prideaux, G. J., et al. (2001). New ages for the last Australian megafauna: Continent-wide extinction about 46, 000 years ago. *Science* 292, 1888–1892. doi:10.1126/science.1060264

Shulmeister, J., Kemp, J., Fitzsimmons, K. E., and Gontz, A. (2016). Constant wind regimes during the last glacial maximum and early holocene: Evidence from little llangothlin lagoon, new england tablelands, eastern Australia. *Clim. Past.* 12 (7), 1435–1444. doi:10.5194/cp-12-1435-2016

Stohl, A., Forster, C., Frank, A., Seibert, P., and Wotawa, G. (2005). Technical note: The Lagrangian particle dispersion model FLEXPART version 6.2. *Atmos. Chem. Phys.* 5 (9), 2461–2474. doi:10.5194/acp-5-2461-2005

Tapper, N., and Hurry, L. (1993). *Australia's weather patterns. An introductory guide*. Victoria: Dellasta Pty Ltd, Mount Waverley.

Tsukamoto, S., Murray, A. S., Huot, S., Watanuki, T., Denby, P. M., Bøtter-Jensen, L., et al. (2007). Luminescence property of volcanic quartz and the use of red isothermal TL for dating tephras. *Radiat. Meas.* 42 (2), 190–197. doi:10.1016/j.radmeas.2006.07.008

Tumney, J. (2001). "Optical dating of megafauna-bearing aeolian deposits in the Corangamite region, Western Victoria," BSc(Honours) Thesis. (Melbourne: University of Melbourne).

White, J. P., and Flannery, T. (1995). Late Pleistocene fauna at spring creek, Victoria: A Re-evaluation. *Aust. Archaeol.* 40, 13–17. doi:10.1080/03122417.1995.11681541

Whittaker, T. E., Hendy, C. H., and Hellstrom, J. C. (2011). Abrupt millennial-scale changes in intensity of Southern Hemisphere westerly winds during marine isotope stages 2–4. *Geology* 39 (5), 455–458. doi:10.1130/g31827.1